AIAA JOURNAL
Vol. 33, No. 11, November 1995

Experimental and Theoretical Study of Wide-Angle Diffuser Flow with Screens

Matthias M. Seltsam*
DLR, German Aerospace Research Establishment, 37073 Göttingen, Germany

A numerical method is modified to enable the computation of diffuser flows containing mesh screens. A Navier–Stokes method with the standard k-ϵ turbulence model is applied. Screen influence on the velocity distribution is demonstrated using flow in a straight duct. A comparison of calculated diffuser flows is made with experimental results. The numerical and experimental investigations on the wide-angle diffuser flow of the transonic wind tunnel at DLR have led to a modification of the actual wind tunnel. An appreciable reduction of spatial velocity disturbances is achieved after realization of the modification.

Nomenclature

c_μ	= constant of k-ϵ turbulence model
H	= height
K	= pressure drop coefficient
k	= turbulent kinetic energy
M	= Mach number
m	= exponent
p	= pressure
p_0	= stagnation pressure
Re_S	= screen Reynolds number
r	= radius coordinate
S	= source term
U	= velocity
U_m	= mean velocity
u, v, w	= velocity components
u', v', w'	= turbulent velocities
x, y, z	= Cartesian coordinate
α	= deflection coefficient
β	= screen porosity
ϵ	= dissipation rate
Θ	= angle between screen normal and upstream flow
μ_k, ν_k	= damping factor in longitudinal and lateral directions
μ_t	= eddy viscosity
ν	= kinematic viscosity
ρ	= density
$\sigma_k, \sigma_\epsilon$	= constants of k-ϵ turbulence model
Φ	= angle between screen normal and downstream flow

Subscripts

i, j, k	= grid indices
K	= related to the pressure drop
sc	= screen
Θ	= dependent on Θ
1, 2	= before, past the screen

I. Introduction

DIFFUSERS are common sections of internal flow systems. They are possible places where disturbances are generated. Proper diffuser design is therefore essential for obtaining uniform flow qualities, particularly in wind tunnels. If wide-angle diffusers are used, design is especially critical. Although many possibilities exist to prevent flow separation occurring in diffusers with angles larger than 12 deg, the installation of screens gives the most uniform outlet velocity profiles. Screens suppress flow separation and reduce flow turbulence at the same time.

Screens must be considered as integral in wide-angle diffuser design. No method, however, for complete computation exists. Diffuser–screen design is still carried out by simple empirical procedures supported by design charts, e.g., given by the Engineering Sciences Data Unit (ESDU)[1] or supported by the data collection of Mehta.[2] Several analytical methods exist to calculate the influence of screens on ducted flows, e.g., the methods of Elder[3] or Owen and Zienkiewicz[4] or others. They obtain realistic results by manipulating the stream function or by employing and modifying the Euler equations, such as Ross,[5] who calculates screened inlet configurations of an indraft wind tunnel. However, present numerical methods are either not qualified to consider the effects of screens (e.g., Nitsche et al.[6] and Kraberger[7]) or they are not qualified to calculate the complex and often detached flow of a diffuser.

This investigation was prompted by the flow in the wide-angle diffuser of the transonic wind tunnel at DLR in Göttingen (TWG). The TWG (Fig. 1) has a test section area of 1×1 m. It operates in a Mach number range from $M = 0.5$–2.0 and in a stagnation pressure range of $p_0 = 30$–145 kPa. The settling chamber contains a cooler, a honeycomb flow straightener, and screens. The diffuser, located upstream, has a mean half-angle of 23 deg and accomplishes the cross-sectional transition from circular to quadratic. No screens had been installed in the diffuser. Flow separation in the diffuser reduces efficiency of the wind tunnel cooler located immediately behind the diffuser and causes nonuniform temperature distribution. Velocity inhomogeneities that affect flow in the test section downstream may also result. The investigations made to improve flow characteristics are reported here.

II. Numerical Investigations

The complete Navier–Stokes equations must be solved to calculate appropriate diffuser flows. A finite volume method based upon the assumption of incompressible flow is used. It employs the k-ϵ turbulence model with the standard constants according to Launder and Spalding.[8] A detailed description is published by Perić et al.[9] and by Kessler et al.[10] The viscous sublayer near the walls is bridged by the wall functions, which assume that the velocity profile near the walls is logarithmic. Although the k-ϵ turbulence model has a number of well-known limitations, the proposed computational method is not intended for extreme accuracy but rather for guiding a proposed change in design. It has the requisite accuracy to demonstrate general effects of screens on ducted flows. Future improvements using refined turbulence models should be easy to integrate.

A. Properties of Wire Screens

Direct representation of a close-meshed screen in a numerical method requires an unacceptable effort. It is not feasible with today's

Presented as Paper 94-2510 at the AIAA 18th Aerospace Ground Testing Conference, Colorado Springs, CO, June 20–23, 1994; received Aug. 16, 1994; revision received Feb. 1, 1995; accepted for publication Feb. 6, 1995.

*Research Scientist, Wind Tunnel Department. Member AIAA.

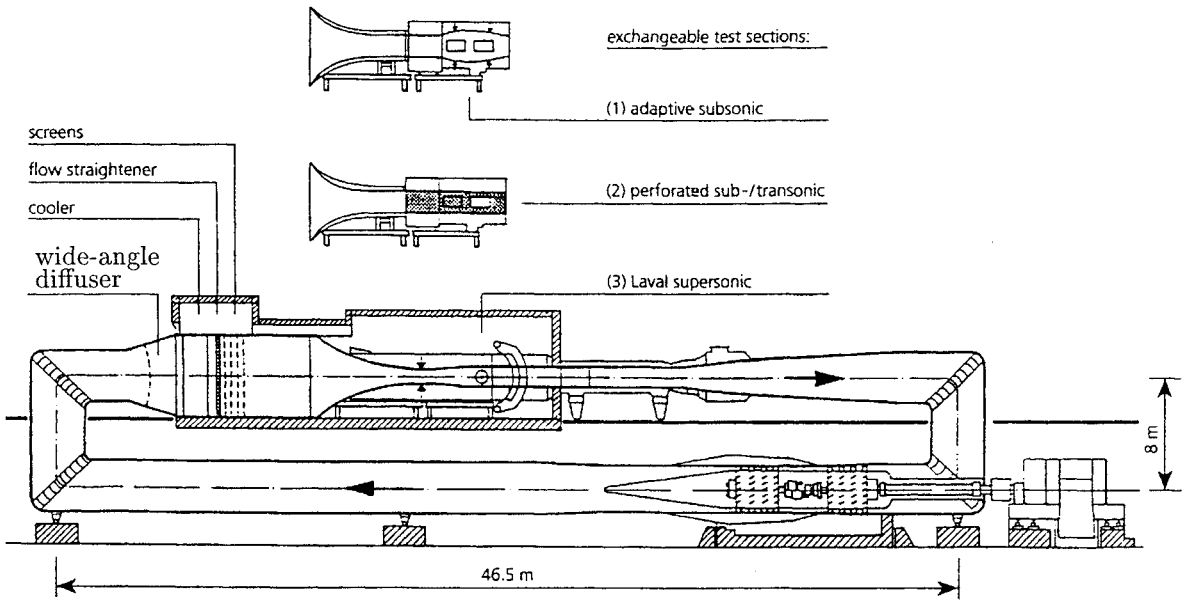

Fig. 1 Transonic wind tunnel at DLR in Göttingen (TWG).

computers. The screen is therefore considered as a discontinuity disk. The numerical method is modified merely by introducing the effects of screens. The various influences of screens on fluid flow are due to two basic effects: The screen causes a local pressure drop Δp_j and a local alteration of the turbulence, expressed by the local turbulent kinetic energy k_j and the local dissipation rate ϵ_j.

Pressure Drop

The local pressure drop across the screen plane is defined as

$$\Delta p_j = K_j \tfrac{1}{2} \rho U_j^2 \tag{1}$$

The pressure drop coefficient K_j is calculated by the formula of Wieghardt.[11] This formula is derived from the resistance of a single cylinder. It is the best validated approximation among all existing attempts to correlate pressure drop and screen porosity:

$$K_j = 6 \frac{1-\beta}{\beta^2} Re_S^{-\frac{1}{3}} \tag{2}$$

This formula is valid in the range of the screen Reynolds number, $Re_S = (ud)/(\nu\beta)$, from 6×10^1 to 6×10^2. The screen porosity β is defined as the fraction of the open area based on frontal projection; d is the wire diameter, and u is the upstream velocity. Above $Re_S = 6 \times 10^2$ the pressure drop remains almost constant according to Cornell,[12] i.e., $K_j = 6(1-\beta)/\beta^2 600^{-1/3}$. Pressure drop diminishes with increasing inclination angle Θ:

$$K_\Theta = K \cos^m \Theta \tag{3}$$

Mehta[13] presents proper data for the definition of the exponent m dependent on screen porosity β. For usage in a numerical method the following analytical relation is defined:

$$m = 2 - \sqrt{(5/3)\beta} \tag{4}$$

Screens are also used for changing flow direction. For small angle between screen and upstream and downstream flows, Θ and Φ, and for moderate porosity ($\beta \cong 0.6$) Mehta[13] gives the empirical relation

$$\alpha \cong \frac{\Phi}{\Theta} = 0.66 + \frac{0.31}{\sqrt{1+K}} \tag{5}$$

This is a modification of Dryden and Schubauer's relation presented by Taylor and Batchelor.[14] It is only applied for the calculation of change in turbulence. Streamline deflection in the numerical procedure is practically the only result due to screen pressure drop.

Alteration of Turbulence

The most important task of screens in wind tunnels is to damp turbulence. Large oncoming eddies are destroyed and smaller, rapidly dissipating eddies are generated. After a short distance flow turbulence becomes isotropic. Depending on screen geometry, screens also work as turbulence generators. As screen porosity decreases, so does the influence of upstream turbulence on the downstream turbulence. Longitudinal motions are generally more damped than lateral ones. Damping factors in longitudinal and lateral direction, μ_k and ν_k, are defined from turbulent velocities before and past the screen:

$$\mu_k = \frac{u_2'}{u_1'} \quad \text{and} \quad \nu_k = \frac{v_2'^2 + w_2'^2}{v_1'^2 + w_1'^2} \tag{6}$$

The mean energy of turbulence upstream is

$$k_1 = \tfrac{1}{2}\left(u_1'^2 + v_1'^2 + w_1'^2\right) \tag{7}$$

The turbulent energy of the downstream flow is determined by the damping factors μ_k and ν_k:

$$k_2 = \tfrac{1}{2}\left[\mu_k u_1'^2 + \nu_k\left(v_1'^2 + w_1'^2\right)\right] \tag{8}$$

The assumption of isotropic turbulence at the screen plane simplifies the relation between the upstream and downstream turbulent energies:

$$k_2 = \tfrac{1}{3} k_1 (\mu_k + 2\nu_k) \tag{9}$$

Taylor and Batchelor[14] derive damping factors μ_k and ν_k for steady and unsteady disturbances. Because steady disturbance relations better approximate experimental finding, they are used in this study:

$$\frac{u_2'}{u_1'} = \frac{1+\alpha-\alpha K}{1+\alpha+K} = \mu_k \tag{10}$$

Lateral disturbances are damped by the factor ν_k, which is equal to the screen deflection coefficient α [Eq. (5)]: $\alpha = \nu_k$.

B. Representation of Screens

The screen is introduced into the numerical method as a local discontinuity. Dependent on upstream flow, the determining values of p, k, and ϵ are altered in the screen plane. The momentum equation is

$$\frac{\partial(\rho U_j U_i)}{\partial x_j} - \frac{\partial}{\partial x_j}\left[(\mu + \mu_t)\frac{\partial U_i}{\partial x_j}\right] = \rho S_{U_i} \tag{11}$$

Pressure drop is represented as an additional source term:

$$S_{U_i} = \frac{\partial}{\partial x_j}\left[(\nu + \nu_t)\frac{\partial U_j}{\partial x_i}\right] - \frac{1}{\rho}\frac{\partial p}{\partial x_i} + S_{\mathrm{sc},j} \tag{12}$$

Using Eqs. (2) and (3), the screen source term becomes

$$S_{\mathrm{sc},j} = -\frac{1}{\rho}\frac{\partial(\Delta p_j)}{\partial x_j} \tag{13}$$

The values of k and ϵ produced by a screen are represented in the transport equations of the k-ϵ model in a similar way:

k-equation:

$$\frac{\partial(\rho U_j k)}{\partial x_j} - \frac{\partial}{\partial x_j}\left[\left(\mu + \frac{\mu_t}{\sigma_k}\right)\frac{\partial k}{\partial x_j}\right] = S_{k,j} \tag{14}$$

ϵ-equation:

$$\frac{\partial(\rho U_j \epsilon)}{\partial x_j} - \frac{\partial}{\partial x_j}\left[\left(\mu + \frac{\mu_t}{\sigma_\epsilon}\right)\frac{\partial \epsilon}{\partial x_j}\right] = S_{\epsilon,j} \tag{15}$$

Dependent on the upstream turbulence values, the source terms S_k and S_ϵ at the screen plane are replaced by screen-determined source terms:

$$S_{k,j} = \frac{\partial(\rho U_j k_{2,j})}{\partial x_j}, \qquad S_{\epsilon,j} = \frac{\partial(\rho U_j \epsilon_{2,j})}{\partial x_j} \tag{16}$$

C. Straight Duct

The representation of screens in the numerical method is examined by calculating the screen effects on the flow of a straight duct. Velocity profiles altered by the screen are emphasized. Effects of different screen resistances and damping potentialities are investigated. Plane, two-dimensional flow is calculated using Cartesian, nonuniform computational grids. Grid lines are concentrated near the screen location in the x direction and near the walls in the y direction. Pressure drop at the screen is added to the source terms of three grid cells behind each other in the ratio of 25%/50%/25% to smooth the screen influence and to avoid difficulties concerning numerical instability. Development of the turbulent quantities is of minor interest in this study. The source terms of the transport equations for the control volumes at screen position are prescribed by values calculated according to Eq. (16).

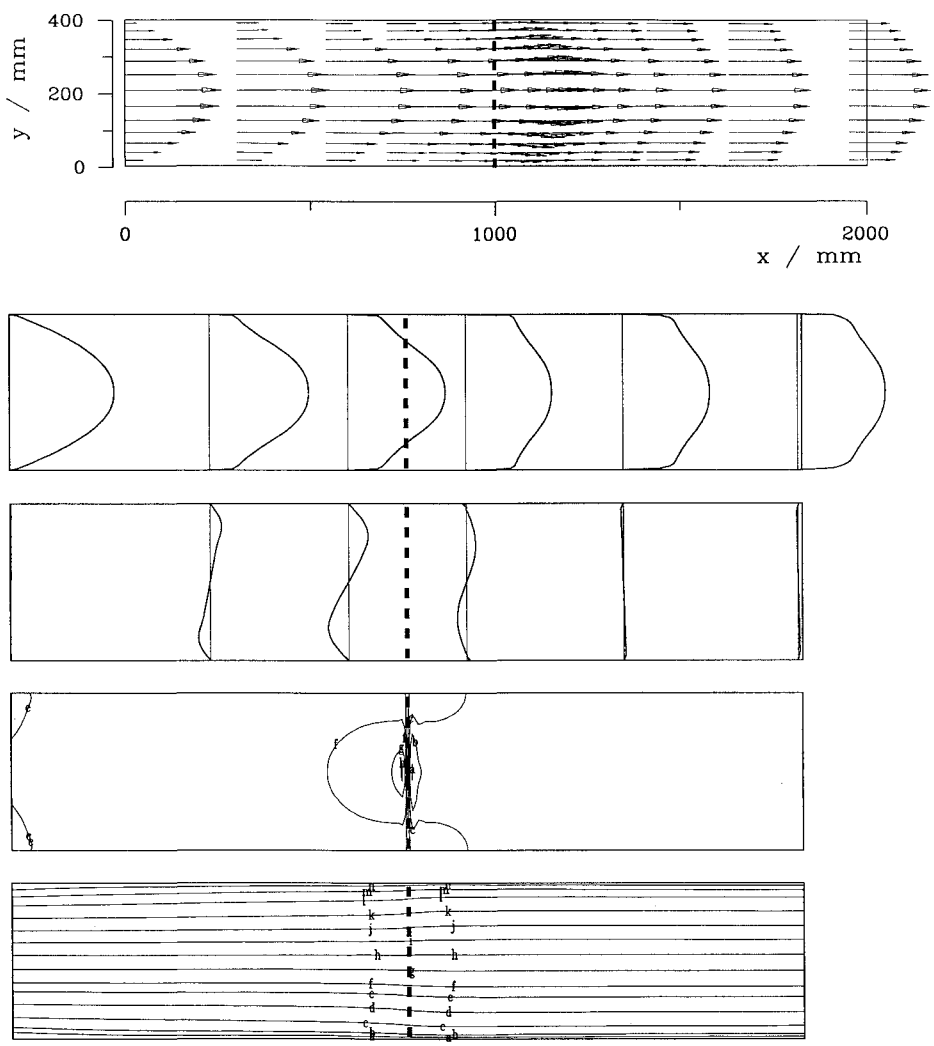

Fig. 2 Straight duct, screen resistance $K = 0.5$: second graph—longitudinal velocity profiles, $u(y)_{max} = 8.00$ m/s; third graph—lateral velocity profiles, $v(y)_{max} = 0.52$ m/s, fourth graph—pressure distribution—(isobars), and fifth graph—streamlines.

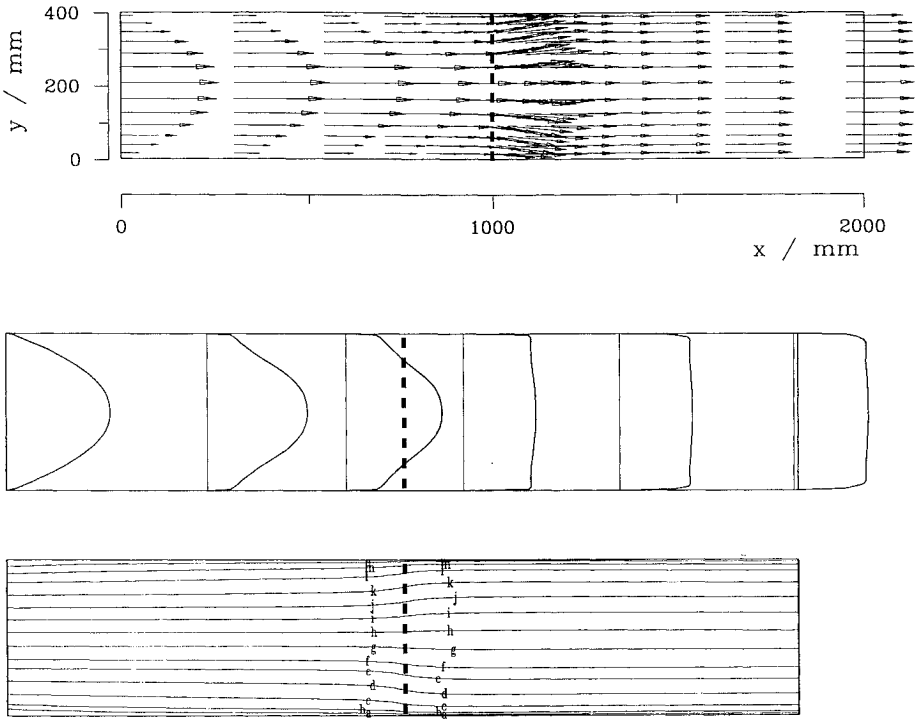

Fig. 3 Straight duct, screen resistance $K = 2.0$: second graph—longitudinal velocity profiles, $u(y)_{max} = 8.00$ m/s, and third graph—streamlines.

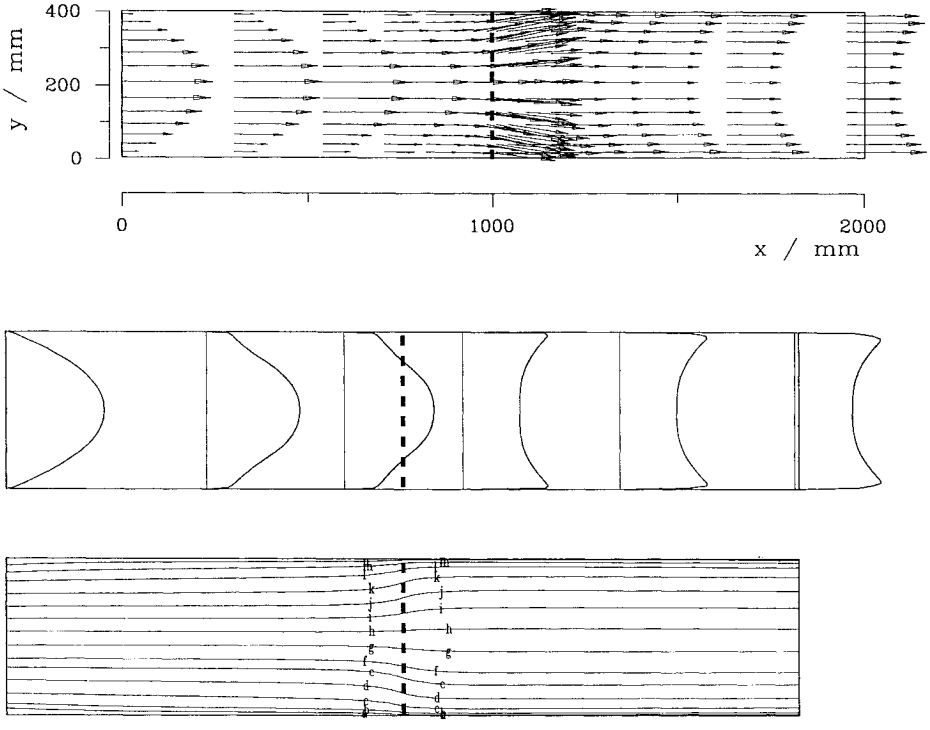

Fig. 4 Straight duct, screen resistance $K = 15.0$: second graph—longitudinal velocity profiles, $u(y)_{max} = 8.41$ m/s, and third graph—streamlines.

The parabolic entry velocity profile selected simulates highly nonuniform flow conditions. Figure 2 shows the influence of a screen with high porosity ($\beta \cong 0.75$) and with a low pressure drop ($K \cong 0.5$). Such a screen is typically applied in settling chambers of wind tunnels to damp flow disturbances. This screen slightly reduces velocity nonuniformities. The isobars show increased pressure in front of the screen center. The duct center, past the screen, shows notable pressure reduction resulting from higher upstream velocities.

An increased pressure drop is considered in Fig. 3. The resistance coefficient of $K = 2.0$ corresponding to the porosity $\beta \cong 0.53$ generates an almost completely homogeneous u-velocity profile. Streamline deflection occurs before and past the screen. Although they produce a high degree of homogeneity, these screens are rarely used due to higher losses and an increased possibility of instability generation, a phenomenon that is observed during the experiments presented in the next sections.

Further increase in screen resistance does not produce an even more uniform velocity profile. With a very high pressure drop ($K \cong 15$ corresponding to $\beta \cong 0.20$) inverted velocity profiles (Fig. 4) are obtained. The streamline graph displays deflection taking place

before the screen due to the "filling effect" and deflection taking place past the screen due to the "acceleration effect." The latter is caused by different local static pressure due to different local pressure drops. Increased upstream velocity leads to reduced local static pressure past the screen and to decelerated flow downstream. Conversely, reduced upstream velocity generates accelerated flow. This "inversion effect" is surprising for the present. It nevertheless corresponds to the experimental results presented in the next section. Some earlier investigators obtained similar experimental results, e.g., Mehta,[13] who detected the "overshoot" in the boundary-layer flow past a screen.

D. Sensitivity to Turbulence Modeling

Proper evaluation of the turbulence quantities past the screen is difficult because simple approximations of turbulence alteration by screens are utilized. Therefore emphasis is laid on resulting velocity profiles under screen influence. The replacement of the source term in the k and ϵ equations by screen-related values in the screen plane causes a step change of the eddy viscosity $\mu_t = \rho c_\mu k^2/\epsilon$. In the vicinity of the screen no attempt is made for modeling the local turbulence accurately, assuming a minor influence of the turbulence across the screen and a dominating influence of the pressure drop of the screen on the downstream velocity profiles. To estimate the influence on turbulence modeling, test calculations have been carried out with different consideration of screen-generated turbulence—with normal turbulence alteration as described in this article (a), with reduced turbulence generation $k_2 = 0$ (b), with increased turbulence generation $k_2 \times 10$ (c), and without turbulence alteration at all $k_2 = k_1$ (d). The influence of the screen pressure drop remains unchanged in all of these cases. We consider the computed velocity profiles of a straight duct one duct width past the screen performing the medium pressure drop $K = 2$ (Fig. 5). Differences in velocity are smaller than 0.50% with the exception of a small region near the walls. With normal turbulence alteration (a), the boundary layer before the screen causes increased velocities past the screen. This corresponds to the overshoot measured by Mehta.[13] Extremely low turbulent energy past the screen (b) leads to lower eddy viscosity and to even more increased velocities. The higher turbulent energy near the walls, produced by manipulated turbulence alteration (c) or, respectively, unchanged k profiles across the screen (d), results in higher eddy viscosity and prevents the increase of the velocities.

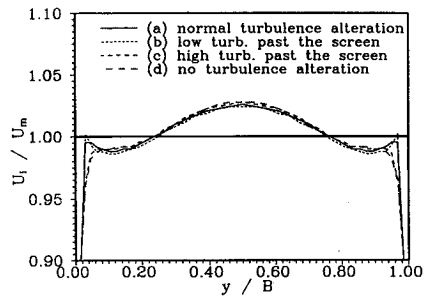

Fig. 5 Velocity distribution one duct width past a screen $K = 2$ for different turbulence alteration.

The most reasonable results are obtained by the actually used method of turbulence alteration. Possible discrepancies in velocities caused by wrong determination of the turbulent quantities are small even in the extreme cases presented here.

E. Diffuser Flow

The representation of a screen in the flow of a straight duct shows reliable results, and so this method is applied to the flow of a diffuser. Figure 6 shows a diffuser flow that is similar to the model diffuser of the TWG diffuser without terminal resistance. (The model diffuser test rig is introduced in the next section.) The flow separates near the diffuser entrance, and a large separation bubble is generated. Results of calculations for a screen at the diffuser exit are presented in Fig. 7. The resistance coefficient of $K = 15$ is equal to the cooler resistance of the actual wind tunnel. Separation is removed

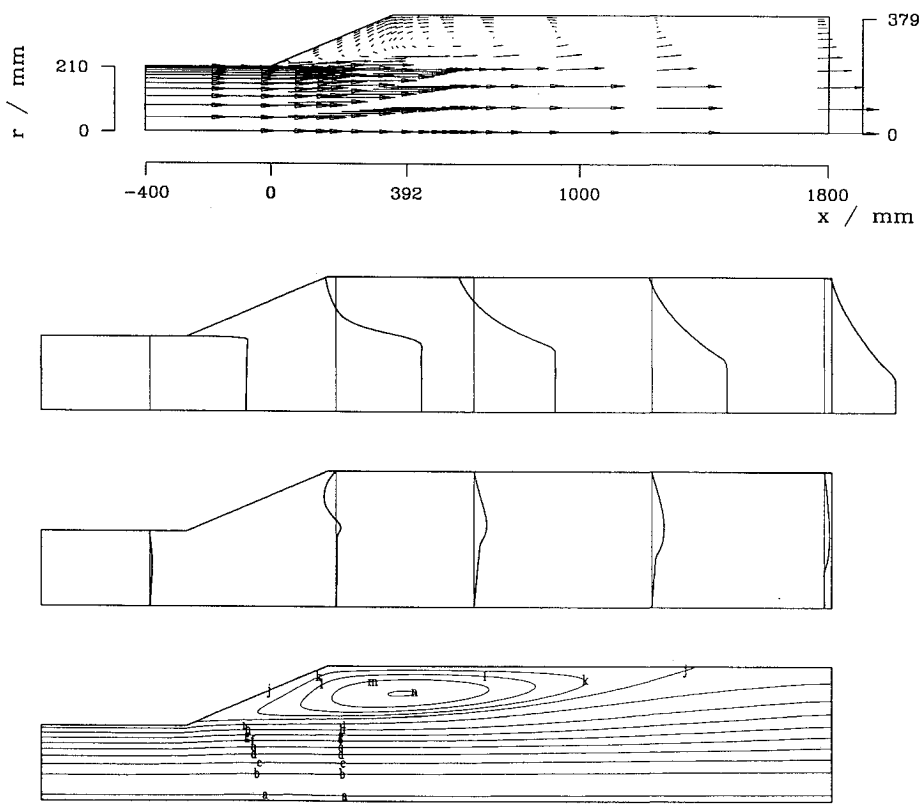

Fig. 6 Axisymmetric diffuser flow, no screen: second graph—longitudinal velocity profiles, $u(y)_{max} = 69.8$ m/s, third graph—lateral velocity profiles, $v(y)_{max} = 15.3$ m/s, and fourth graph—streamlines.

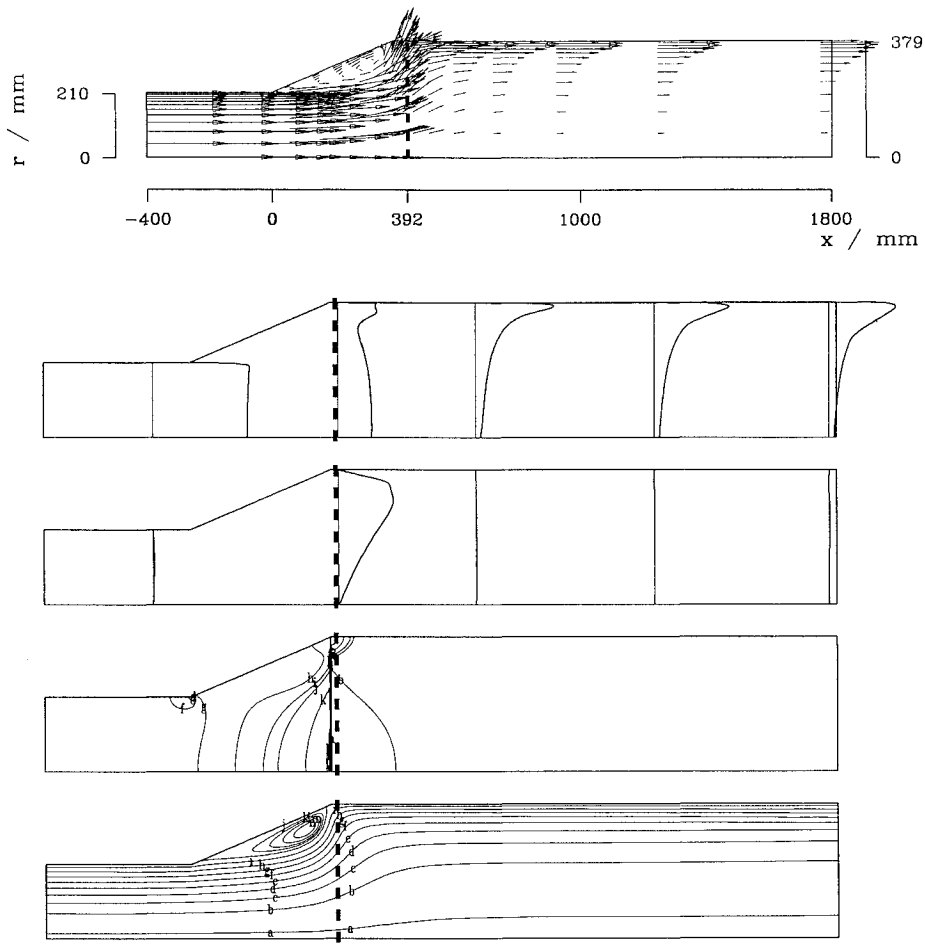

Fig. 7 Axisymmetric diffuser flow with screen (terminal resistance, $K = 15$, $x = 392$ mm): second graph—longitudinal velocity profiles, $u(y)_{max} = 70.6$ m/s, third graph—lateral velocity profiles, $v(y)_{max} = 46.4$ m/s, fourth graph—pressure distribution, and fifth graph—streamlines.

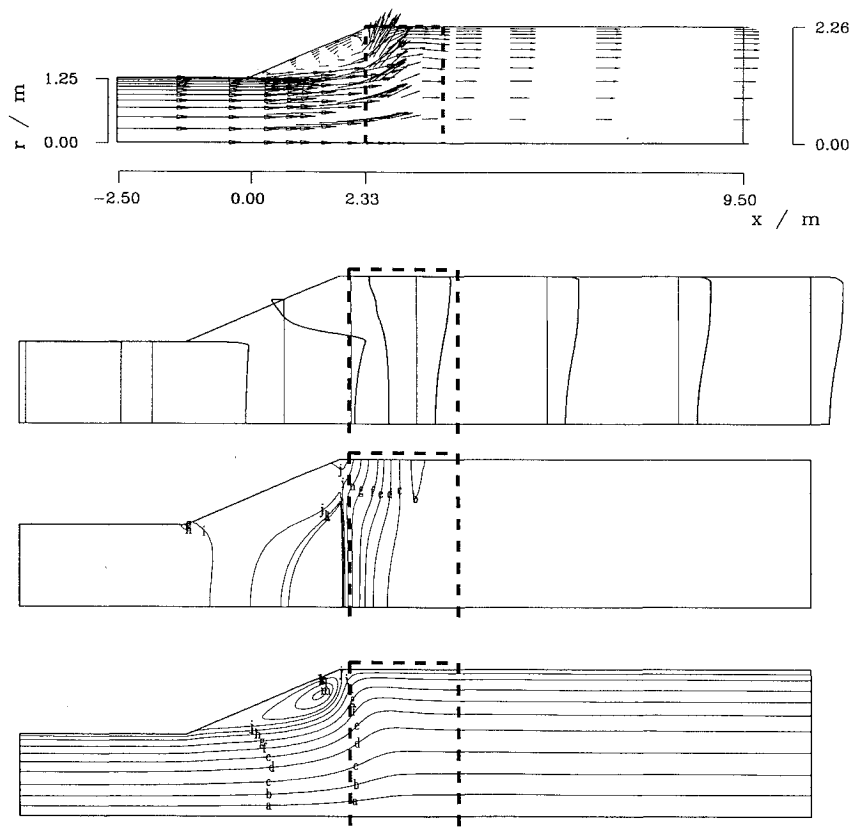

Fig. 8 Axisymmetric diffuser flow, cooler at the end (TWG configuration): second graph—longitudinal velocity profiles, $u(y)_{max} = 40.8$ m/s, third graph—pressure distribution, and fourth graph—streamlines.

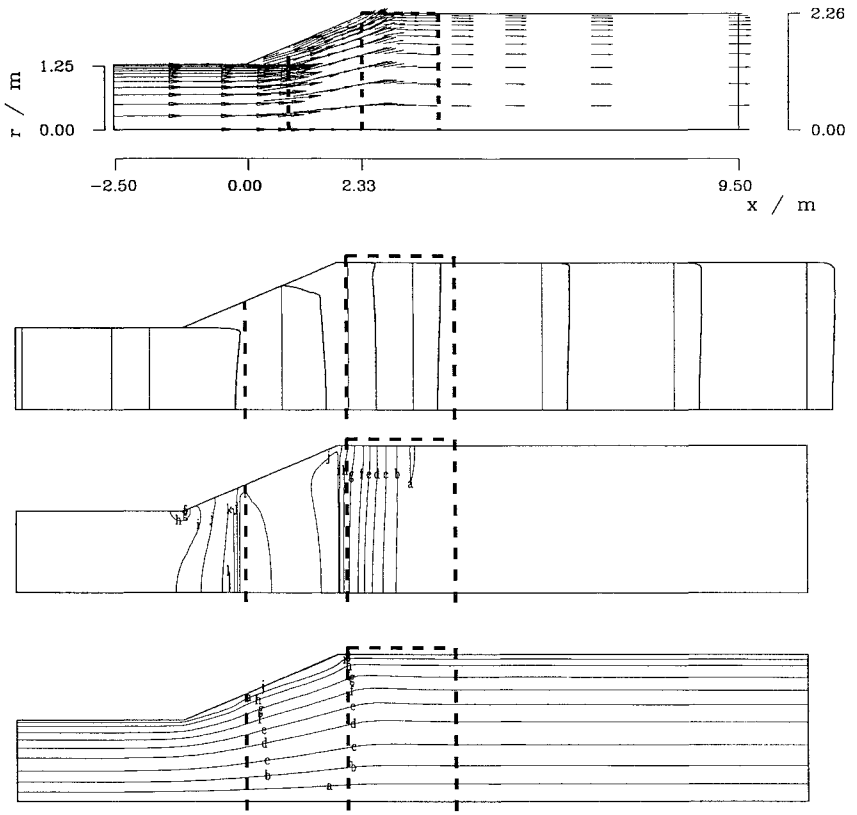

Fig. 9 Axisymmetric diffuser flow with cooler and screen (TWG configuration after modification): second graph—longitudinal velocity profiles, $u(y)_{max}$ = 43.9 m/s, third graph—pressure distribution, and fourth graph—streamlines.

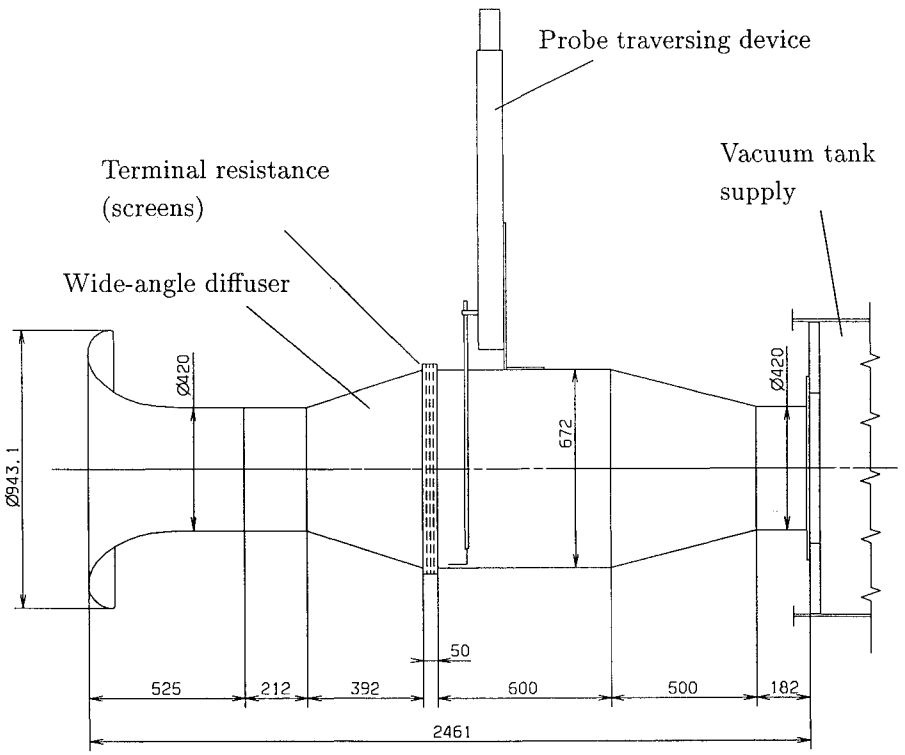

Fig. 10 Model diffuser test rig (measuring units in mm).

at the screen location, but a separation bubble remains in front of the screen. A remarkable change in the velocity profiles is generated by the screen resistance due to the streamline deflection. Enormous increase of the velocities past the screen near the wall corresponds to the results obtained for a straight duct.

For the determination of the diffuser flow of the actual wind tunnel, the pressure drop of the cooler, which is located at the exit as terminal resistance, must be considered in an appropriate way. That means the pressure drop must be distributed in the x direction. Figure 8 displays the flow for the dimensions of the TWG. Separation persists in the diffuser. Nevertheless, the outlet velocity profiles show increased homogeneity. Nearly uniform velocity profiles are obtained by adding a screen in the diffuser (Fig. 9). Integration of a screen ($K = 1.90$) into the wind tunnel diffuser leads to nearly

optimal diffusion. This modification has been accepted into practice at the TWG.

III. Model Study and Validation of Modified Numerical Method

Existing analytical methods to improve the flow of the TWG diffuser are suggested to be not reliable enough. Therefore a test rig (Fig. 10) at a scale of 1:5.95 has been built to test various modifications in the diffuser. For each version wall static pressures are measured to determine the local pressure recovery. Wool tufts enable visualization of the flow. A traversing Prandtl probe past the screens representing the wind tunnel cooler yields the most interesting data. The velocity is determined using the local total pressure and the local static pressure. It is plotted against the tunnel height related to the mean velocity in the section plane. It is possible to transpose the traversing device to record four different measuring lines side by side—one line of the probe position (PP) in the middle of the duct (PP0, thick plotted), one near the wall (PP3), and two between them (PP1 and PP2).

The results for the empty diffuser (Fig. 11 top) show increased velocities in the center and also increasing velocities near the walls. The velocity distribution is highly nonuniform.The measured data for each line seem to be noisy and scattered. Measurements for several of the different versions are repeated under the same conditions, and almost exactly the same results are always obtained. Therefore it can be stated that these small-scale disturbances are location dependent and not time dependent.This phenomenon occurs due to the instability effect also observed during tests in the actual wind tunnel.

Several types of guide vanes are tested in the diffuser, as well as several screens and screen combinations. The screens can be build in at two positions: at the inlet ($x = 0$ mm, curved screens) and at two-thirds the length from the inlet of the diffuser ($x = 130$ mm). Best results are achieved using a screen of $K = 1.90$ at $x = 130$ mm. The velocity distribution (Fig. 11 bottom) with this moderate additional loss is more uniform, although a slight increase near the walls persists.

Experimental values for the middle measuring line of the downstream duct at various distances from the diffuser, with and without a screen, are compared with numerical results plotted for different

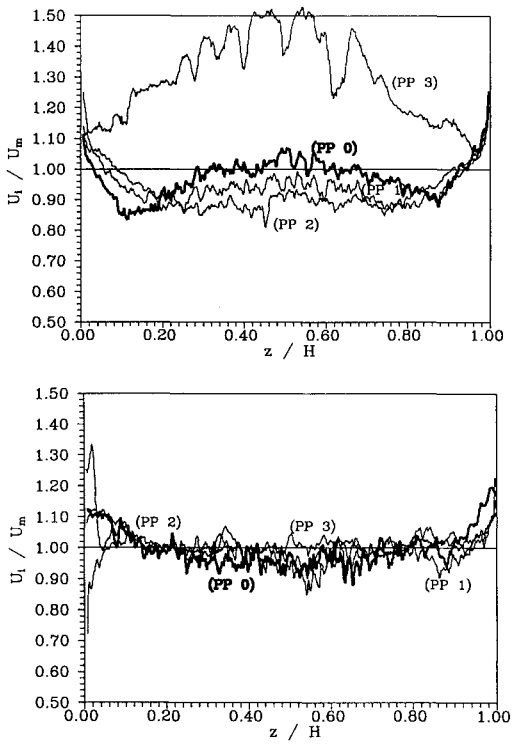

Fig. 11 Velocity distribution past the terminal resistance (four measuring lines): top graph—empty diffuser, and bottom graph—screen in the diffuser.

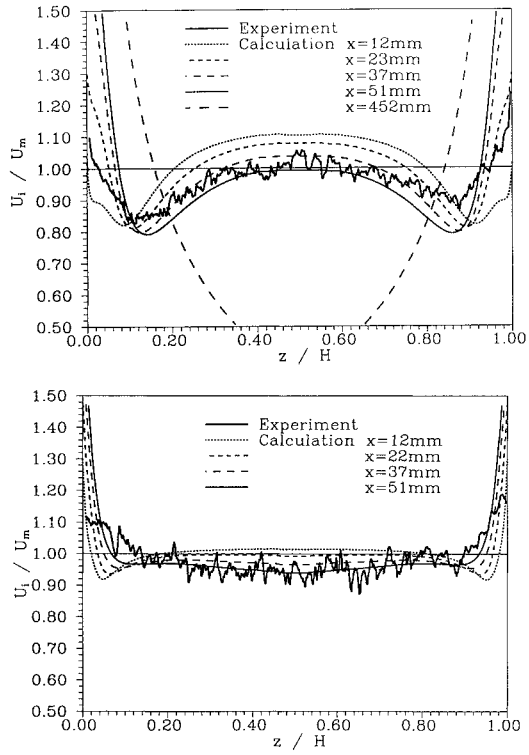

Fig. 12 Comparison calculation—experiment: velocity distribution past the terminal resistance (on the centerline: PP0), calculated velocity profiles of five (four) different distances past the screen: top graph—empty model diffuser, and bottom graph—screen in the model diffuser.

distances from the screen (Fig. 12). The traversing probe has been about 50 mm away from the screen.

Agreement is quite appreciable, though the geometries are different. The tested diffuser performs the transition from circular to quadratic cross-sectional area in contrast to the axisymmetric design of the calculated diffuser. A large computed increase in velocity near the walls occurs because of the absence of the wind-tunnel nozzle in the computational grid, because of three-dimensional effects in the tested diffuser and because of deficiencies in the representation of the screen in the numerical method. The screen is considered in a very narrow region, i.e., over three grid cells. The simulation of the cooler shows that the velocity profiles become more uniform with a distributed pressure drop. Therefore more about the generation of the pressure drop must be known to achieve a more realistic consideration of screens.

IV. Investigations in the Wind Tunnel

Results of both numerical and experimental investigations indicate a modification for the wind-tunnel diffuser. Pre- and postmodification measurements of velocity distributions have been carried out. Settling chamber design permits measurements only at the end, in front of the nozzle (Fig. 13). A traversing probe provides data acquisition across the whole cross section. The section where measurements are taken is located past all settling chamber installations provided to damp disturbances. Nevertheless, the influence of the flow separation in the diffuser is proved.

Velocity profiles measured on the horizontal in the middle of the duct show large-scale disturbances due to detached diffuser flow (Fig. 14 top). After installing the specified screen in the diffuser, the flow is attached and these disturbances are removed (Fig. 14 bottom). The velocity disturbances are reduced from $\pm 2\%$ to $\pm 0.5\%$. The remaining small-scale disturbances are caused by a so far insufficiently explained screen effect. They are steady, only location dependent. All measurements have been repeated four times with insignificant deviation. Mutual coalescence of the jets emerging from screens with low porosity is responsible for the obtained steady structure. This effect usually called instability is clearly demonstrated by Bradshaw[15]; it has not been expected past the employed screen with a porosity of $\beta = 0.59$.

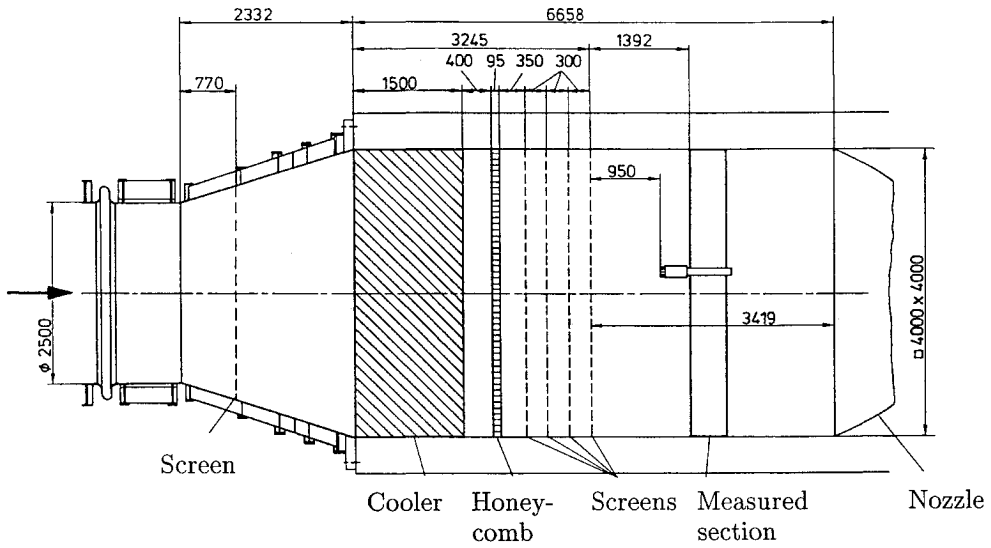

Fig. 13 Settling chamber of the TWG (measuring units in mm).

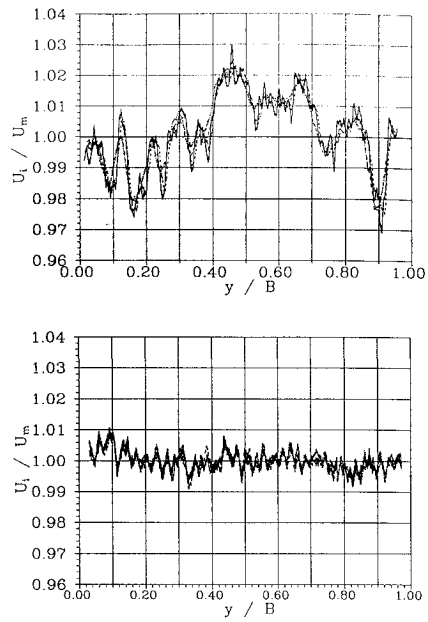

Fig. 14 Measured velocity distribution in the settling chamber of the TWG (four measuring lines of the same flow situation overlap each other): top graph—empty diffuser, and bottom graph—specified screen in the diffuser.

V. Conclusions

Extensions have been made on a numerical method to account for screens installed in an internal flow system. Screens or similar installations are necessary in many flow systems, e.g., in wide-angle diffusers to obtain uniform downstream velocity profiles. The employed method utilizing the Navier–Stokes equations with the standard k-ϵ turbulence model permits critical assessment of separated flows. Representation of a screen is made possible by consideration of the local pressure drop and by consideration of the local alteration of the turbulent quantities, k and ϵ. Computed velocity profiles of the diffuser show appreciable agreement with the results of the model study, which was aimed to improve flow in the wide-angle diffuser of the TWG.

The method presented here can be used to design new wide-angle diffusers as well as to improve existing flow systems. The turbulence alteration past screens used in settling chambers of wind tunnels and screen efficiency to damp small-scale disturbances cannot yet be predicted by the numerical method. Assumptions made to derive the influence of screens on turbulent quantities are still simple. Local effects of screens on turbulence alteration as well as on spatial pressure drop must be even better understood.

A model study is also carried out to find an appropriate modification for the wide-angle diffuser of the TWG, to remove flow separation, and to generate a uniform downstream velocity profile. The numerical and experimental procedures both indicate that a specified screen should be installed in the diffuser. This has been done and a distinct reduction of velocity disturbances is demonstrated.

Acknowledgment

Support by R. Kessler, DLR, for screen representation in the numerical method is gratefully acknowledged.

References

[1]Thomson, N., et al., *Performance of Conical Diffusers in Incompressible Flow*, Engineering Sciences Data Unit, ESDU 73024, London, 1973.

[2]Mehta, R. D., "The Aerodynamic Design of Blower Tunnels with Wide-Angle Diffusers," *Progress in Aerospace Sciences*, Vol. 18, No. 1, 1977, pp. 59–120.

[3]Elder, J. W., "Steady Flow Through Non-Uniform Gauzes of Arbitrary Shape," *Journal of Fluid Mechanics*, Vol. 5, Pt. 3, 1959, pp. 355–368.

[4]Owen, P. R., and Zienkiewicz, H. K., "The Production of Uniform Shear Flow in a Wind Tunnel," *Journal of Fluid Mechanics*, Vol. 2, Pt. 6, 1957, pp. 521–531.

[5]Ross, J. C., "Theoretical and Experimental Study of Flow-Control Devices for Inlets of Indraft Wind Tunnels," NASA TM 100050, Sept. 1989.

[6]Nitsche, W., Nasseri, M., and Bartsch, P., "Investigation on Turbulent Transport Processes in Relaxing Diffuser Flows," *Engineering Turbulence Modelling and Experiments*, Vol. 2, Elsevier, Amsterdam, 1993, pp. 479–488.

[7]Kraberger, G., "Berechnung der Strömung in Windkanaldiffusoren unter Berücksichtigung der Sekundärströmung zweiter Art," *Zeitschrift für Flugwissenschaften und Weltraumforschung*, ZFW 14, 1990, pp. 361–372.

[8]Launder, B. E., and Spalding, D. B., "The Numerical Computation of Turbulent Flows," *Computer Methods in Applied Mechanics and Engineering*, No. 3, 1974, pp. 269–289.

[9]Perić, M., Kessler, R., and Scheuerer, G., "Comparison of Finite-Volume Numerical Methods with Staggered and Colocated Grids," *Computers and Fluids*, Vol. 16, No. 4, 1988, pp. 389–403.

[10]Kessler, R., Perić, M., and Scheuerer, G., "Solution Error Estimation in the Numerical Predictions of Turbulent Recirculating Flows," *Validation of Computational Fluid Dynamics*, Conference Proceedings No. 437, AGARD, 1989.

[11]Wieghardt, K. E. G., "On the Resistance of Screens," *Aeronautical Quarterly*, Vol. 4, Feb. 1953, pp. 186–192.

[12]Cornell, W. G., "Losses in Flow Normal to Plane Screens," *Transactions of the American Society of Mechanical Engineer*, Vol. 80, May 1958, pp. 791–799.

[13]Mehta, R. D., "Turbulent Boundary Layer Perturbed by a Screen, *AIAA Journal*, Vol. 23, No. 9, 1985, pp. 1335–1342.

[14]Taylor, G. I., and Batchelor, G. K., "The Effect of Wire Gauze on Small Disturbances in a Uniform Stream," *Quarterly Journal of Mechanics and Applied Mathematics*, Vol. 2, Pt. 1, 1949, pp. 1–29.

[15]Bradshaw, P., "The Effect of Wind-Tunnel Screens on Nominally Two-Dimensional Boundary Layers," *Journal of Fluid Mechanics*, Vol. 22, Pt. 4, 1965, pp. 679–688.